

RESEARCH ARTICLE

Crystalline aliphatic polyesters from eight-membered cyclic (di)esters

Xiaoyan Tang^{1,2}  | Changxia Shi² | Zhen Zhang² | Eugene Y.-X. Chen² 

¹Beijing National Laboratory for Molecular Sciences, Key Laboratory of Polymer Chemistry and Physics of Ministry of Education, Center for Soft Matter Science and Engineering, College of Chemistry and Molecular Engineering, Peking University, Beijing, China

²Department of Chemistry, Colorado State University, Fort Collins, Colorado, USA

Correspondence

Xiaoyan Tang and Eugene Y.-X. Chen, Department of Chemistry, Colorado State University, Fort Collins, CO 80523-1872, USA.

Email: xiaoyan.tang@pku.edu.cn and eugene.chen@colostate.edu

Funding information

National Natural Science Foundation of China, Grant/Award Number: 52173093; National Science Foundation, Grant/Award Number: NSF-1955482; Peking University Ge Li and Ning Zhao Life Science Research Fund for Young Scientists

Abstract

Ring-opening polymerization (ROP) of lactones or cyclic (di)esters is a powerful method to produce well-defined, high-molecular-weight (bio)degradable aliphatic polyesters. While the ROP of lactones of various ring sizes has been extensively studied, the ROP of the simplest eight-membered lactone, 7-heptanolactone (7-HL), has not been reported using metal-based catalysts. Accordingly, this contribution reports the ROP of 7-HL via metal-catalyzed coordinative-insertion polymerization to the corresponding high-molecular-weight polyester, poly(7-hydroxyheptanoate) (P7HHp). The resulting P7HHp is a semi-crystalline material, with a T_m of 68 °C, which is ~10 °C higher than poly(ϵ -caprolactone) derived from the seven-membered lactone. Mechanical testing showed that P7HHp is a hard and tough plastic, with elongation at break >670%. P7HHp-based polyesters with higher T_m values have been achieved through stereoselective copolymerization of 7-HL with an eight-membered cyclic diester, racemic dimethyl diolide (*rac*-8DL^{Me}), known to lead to high T_m poly(3-hydroxybutyrate) (P3HB). Notably, catalyst's strong kinetic preference for polymerizing *rac*-8DL^{Me} over 7-HL in the 1/1 comonomer mixture rendered the formation of di-block copolymer P3HB-*b*-P7HHp, showing two crystalline domains with T_{m1} ~ 65 °C and T_{m2} ~ 160 °C. Semi-crystalline random copolymers with T_m up to 164 °C have also been obtained by adjusting copolymerization conditions. Mechanical testing showed that P3HB-*b*-P7HHp can synergistically combine the high modulus of isotactic P3HB with the high ductility of P7HHp.

KEYWORDS

aliphatic polyesters, eight-membered cyclic (di)esters, metal-based catalysts, ring-opening polymerization

1 | INTRODUCTION

Aliphatic polyesters are the most promising members of biodegradable polymers, considered to be the more sustainable alternatives to petroleum-based, non-degradable commodity polymers such as polyolefins.^{1–4} There are two main pathways to produce polyesters: (1) polycondensation of A₂

monomers such as diacids or diesters with B₂ monomers such as diols, or polycondensation of AB monomers such as hydroxyacids or hydroxyesters, which demands high energy input to continuously remove co-products such as water and alcohols, the process of which becomes even more difficult as viscosity increases, thus limiting its ability to produce high-molecular-weight polymers; and (2) ring-opening

polymerization (ROP) of cyclic esters (lactones) or diesters (lactides, diolides), which provides a kinetically fast and structurally controlled chain-growth method to produce well-defined, high-molecular-weight polyesters. Therefore, the ROP of lactones of various ring sizes by metal-based, organic or enzymatic catalysts has been extensively studied, offering polyesters with diverse properties.^{5–17} Moreover, ring-opening copolymerization of different cyclic (di)esters has also been used to produce copolymers, and their microstructures (block, gradient, or random) and thus properties can be modulated by varying the monomers ratio and/or other polymerization conditions.^{18–20}

Among several different polymerization techniques, metal-catalyzed ROP via a coordination-insertion mechanism is often considered to be the most efficient method for cyclic (di)esters polymerization.^{6–12} Particularly, specifically designed metal complexes that are structurally well matched with chiral monomers could bring about high stereoselectivity for the synthesis of stereoregular, crystalline polymers. Take four- and eight-membered cyclic esters as an example, the ROP of *rac*- β -butyrolactone (*rac*- β -BL) can produce either highly syndiotactic poly(β -BL) (PBL) with P_r (defined as the probability of racemic linkages between adjacent monomer units) up to 0.95 using discrete yttrium complexes supported by tetradentate, dianionic alkoxy-amino-bis(phenolate) [O^- , N , O , O^-] ligands,^{21–24} or iso-enriched PBL ($P_m \leq 0.85$) with alkyl aluminoxanes,^{25–27} chiral initiator by in-situ reaction of $ZnEt_2$ with (*R*)(–)-3,3-dimethyl-1,2-butanediol,²⁸ chromium(III) salophen complexes,²⁹ grafted neodymium borohydrides onto silica,³⁰ and salen-ligated rare-earth metal amide complexes.³¹ PBL is chemically equivalent of poly(3-hydroxybutyrate) (P3HB), the simplest, more important member of the large biodegradable polyhydroxyalkanoate (PHA) family.^{32–43} More recently, catalyzed chemical synthesis of perfectly isotactic P3HB has been realized via the stereoselective ROP of the racemic eight-membered diolide (*rac*-8DL^{Me}), using racemic salen-yttrium or lanthanum catalysts **1–2**.^{44,45} In particular, kinetic resolution polymerization of *rac*-8DL^{Me} with enantiomeric catalysts (*R,R*)-**1** and (*S,S*)-**1** produced enantiomeric poly[(*S*)-3HB] and poly[(*R*)-3HB] with a high melting temperature (T_m) of 175 °C. Moreover, copolymerization *rac*-8DL^{Me} with longer alkyl substituted diolide monomers, *rac*-8DL^R (R = Et, ⁿBu), or benzyl substituted monomer, *meso*-8DL^{Bn}, can produce crystalline isotactic PHA copolymers with promising polyolefin-like thermal and mechanical properties.^{46,47}

For lactones without stereogenic centers, semi-crystalline polyesters can be readily obtained from the ROP of the most common five-, six-, and seven-membered lactones.⁷ For example, five-membered γ -butyrolactone (γ -BL)

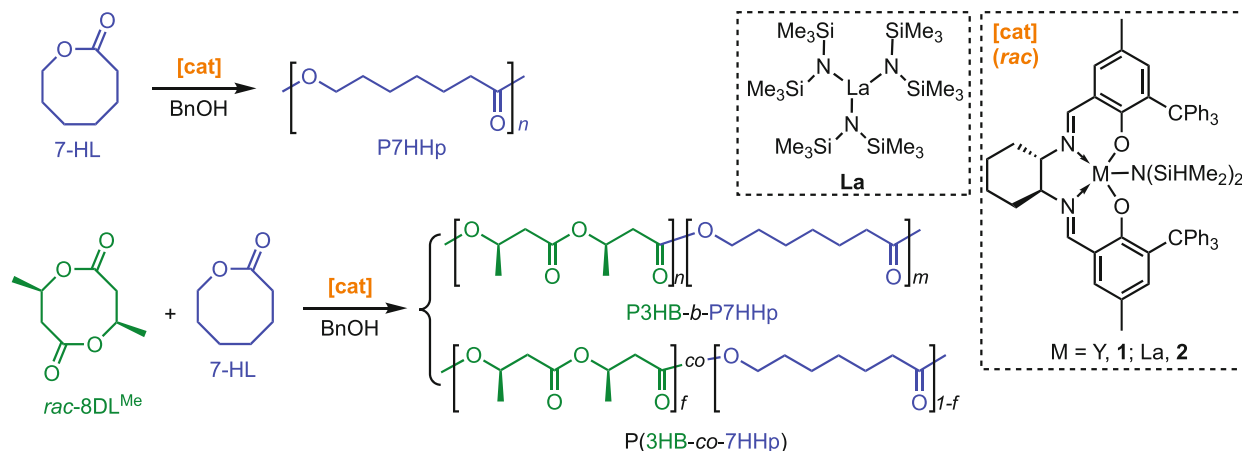
with negligible strain energy can be effectively polymerized under suitable conditions and using rare-earth metal catalysts, $La[N(SiMe_3)_2]_3$ and yttrium complex supported by tetradentate, dianionic alkoxy-amino-bis(phenolate) [O^- , N , O , O^-] ligands, producing semi-crystalline poly(γ -butyrolactone) (P γ BL) with T_m of ~ 60 °C.⁴⁸ A large number of initiators or catalysts, encompassing virtually the entire periodic table, have also been employed for the ROP of ϵ -caprolactone (ϵ -CL), a seven-membered lactone. The intensive investigation in this front is largely due to the fact that the corresponding poly(ϵ -caprolactone) (PCL) is an important class of biodegradable and biocompatible polymer that is semi-crystalline with a modest T_m of ~ 58 °C and a low T_g of about -58 °C and can be readily degraded by aerobic and anaerobic microorganisms.^{9,49–56}

Although the ROP of lactones of various ring sizes has been extensively investigated by metal-based catalysts, the ROP of eight-membered lactone, 7-heptanolactone (7-HL), has not been reported using this polymerization methodology to the corresponding high-molecular-weight poly(7-hydroxyheptanoate) (P7HHp). It should be noted here that lipase-catalyzed ROP of 7-HL by Novozym 435 was reported, yielding P7HHp as a semi-crystalline material with a T_m of 65 °C, but the number-average molar mass (M_n) of P7HHp by this method reached only to 23.6 kg/mol and the P7HHp also had a high dispersity of $\mathcal{D} = 2.8$.⁵⁷ Here we utilized the metal-catalyzed coordination-insertion polymerization strategy to produce P7HHp with high molar mass (M_n up to ~ 100 kg/mol) and a T_m of 68 °C, which is ~ 10 °C higher than PCL. The catalysts employed for the ROP of 7-HL are discrete $La[N(SiMe_3)_2]_3$ and salen-ligated yttrium and lanthanum complexes (Scheme 1), which have been shown to be highly active toward ROP of lactones such as ϵ -CL, γ -BL, MBL, and so forth.^{48,58,59} Moreover, to increase the T_m value of P7HHp-based polyesters, thus widening application windows, the stereoselective copolymerization of 7-HL with *rac*-8DL^{Me} was investigated to produce copolymers of P7HHp and P3HB with T_m up to 164 °C.

2 | RESULTS AND DISCUSSION

2.1 | Homopolymerization of 7-HL and thermal and mechanical properties of P7HHp

The catalytic behavior of complexes $La[N(SiMe_3)_2]_3$ (**La**) and **1–2** toward 7-HL polymerization (Table 1) was investigated firstly. Without benzyl alcohol (BnOH) co-initiator, complex $La[N(SiMe_3)_2]_3$ alone showed high activities toward the ROP of 7-HL, achieving near-quantitative



SCHEME 1 ROP of 7-HL and copolymerization of 7-HL with *rac*-8DL^{Me} by metal-based complexes

TABLE 1 Results of 7-HL polymerization by precatalysts La[N(SiMe₃)₂]₃ and 1-2^a

Run	Catalyst (Cat)	[7-HL]/[Cat]/[BnOH]	Time (min)	Conv. ^b (%)	$M_{n,calcd}$ ^c (kg/mol)	M_n ^d (kg/mol)	\bar{D} ^d (M_w/M_n)
1	La	800/1/0	2	98	33.7	26.1	2.47
2	La	2000/1/0	4	96	82.2	35.8	2.30
3	La	800/1/3	1	100	34.3	11.5	1.10
4	La	2000/1/3	4	>99	84.7	50.8	1.30
5	1	400/1/1	25	100	51.4	12.0	1.54
6	1	800/1/1	50	96	98.5	17.5	1.82
7	2	800/1/1	2	100	103	66.0	1.60
8	2	2000/1/1	4	100	256	93.4	1.48

^aConditions: 7-HL = 0.256 g (2 mmol), $V_{solvent}$ = 0.76 mL, [7-HL] = 2.0 M, dichloromethane (DCM) as the solvent, BnOH as the initiator, the catalyst and initiator amount varied according to the [7-HL]/[Cat]/[BnOH] ratio, room temperature.

^bConversions of 7-HL measured by ¹H NMR spectra of the quenched solution in benzoic acid/chloroform.

^c $M_{n,calcd}$ = MW(7-HL) × [7-HL]/[cat] × conv (%) + MW of chain-end groups.

^dWeight-average molar mass (M_w), number-average molar mass (M_n), and dispersity (\bar{D} = M_w/M_n) determined by size exclusion chromatography (SEC) coupled with an 18-angle light scattering detector at 40 °C in chloroform.

conversion in minutes and giving P7HHp with M_n = 26.1–35.8 kg/mol but high \bar{D} values ranging from 2.30 to 2.47 (runs 1–2, Table 1). When BnOH (3 equiv.) was introduced into the system that reacts rapidly with lanthanide (Ln) amides via in situ alcoholysis to generate the corresponding Ln alkoxides,⁴⁸ which usually exhibit superior performances and mediate more controllable ROP of cyclic esters than the corresponding amido analogues, the ROP produced P7HHp with lower \bar{D} values of 1.10–1.30 (runs 3–4, Table 1). The salen-ligated lanthanum complex **2** in combination with BnOH exhibited higher activity than the yttrium analogue **1** (runs 7–8 vs 5–6, Table 1), affording P7HHp with M_n up to 93.4 kg/mol. Overall, all complexes showed high activities, but the relatively broad dispersities of the resulting P7HHp and discrepancies between calculated and measured molar mass are likely due to the transesterification during polymerization process.

The thermal properties of P7HHp characterized by differential scanning calorimetry (DSC) revealed a T_m of 68 °C (Figure 1A), which is ~10 °C higher than PCL derived from the seven-membered lactone, ϵ -CL. The thermogravimetric analysis (TGA) and relative derivative thermogravimetry (DTG) curves of P7HHp showed a high initial degradation temperature (T_d , defined by the temperature of 5% weight loss) of 353 °C, and a T_{max} (the temperature at the maximum decomposition rate) of 397 °C (Figure 1B). Tensile testing of dog-bone-shaped P7HHp specimens (M_n = 93.4 kg/mol, prepared by [7-HL]/[**2**] = 2000/1; run 8, Table 1), processed by compression molding, yielded a stress/strain curve (Figure 2) showing an ultimate tensile strength (σ_B) of 35.3 ± 2.8 MPa, Young's modulus (E) of 628 ± 4 MPa, and impressive elongation at break (ϵ_B) of 672 ± 49%. Thus, P7HHp showed somewhat higher Young's modulus, slightly lower tensile strength, and comparable

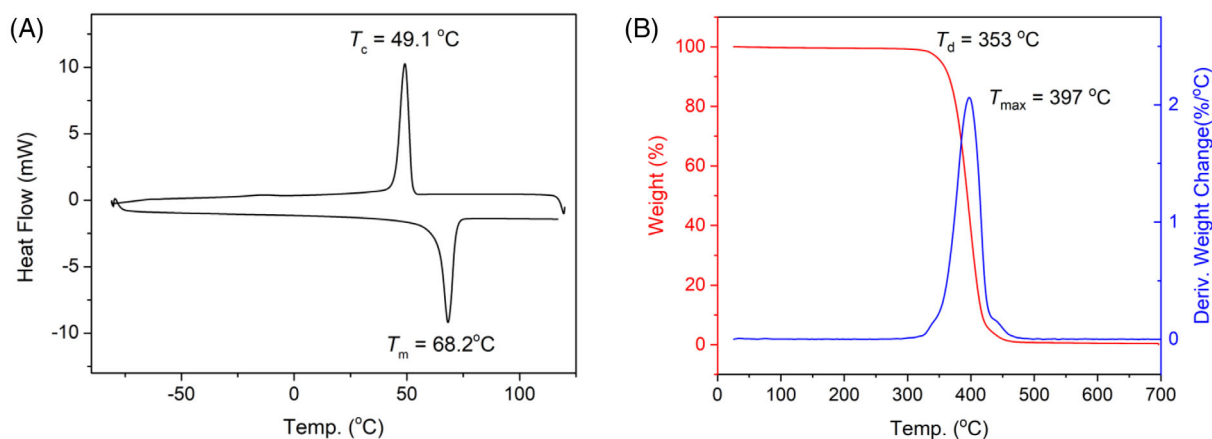


FIGURE 1 (A) DSC curve and (B) TGA (red) and DTG (blue) curves of P7HHp produced by $[\text{La}[\text{N}(\text{SiMe}_3)_2]_3$ (run 4, Table 1)

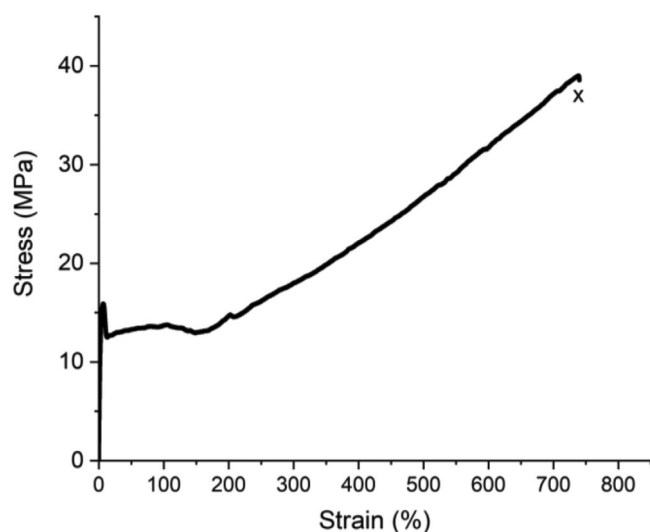


FIGURE 2 Stress-strain curve (10 mm/min, ambient temperature) of P7HHp ($M_n = 93.4$ kg/mol). Break point indicated by “x”

elongation at break, when compared to PCL even with considerably high molar mass of $M_n = 204$ kg/mol, which had $\sigma_B = 39.6 \pm 1.4$ MPa, $E = 587 \pm 19$ MPa, and $\epsilon_B = 698 \pm 30\%$.⁶⁰

2.2 | Copolymerization of 7-HL with $\text{rac-8DL}^{\text{Me}}$

C_2 -ligated chiral complexes **1–2** have been shown to catalyze stereoselective ROP of $\text{rac-8DL}^{\text{Me}}$ to crystalline P3HB with perfect isotacticity ($P_m > 0.99$, $[mm] > 99\%$) and high molar mass.^{44,45} Thus, these two complexes were chosen for investigation of the copolymerizations of 7-HL with $\text{rac-8DL}^{\text{Me}}$. Selected copolymerization results and detailed conversion data are summarized in Table 2

and Table S1, respectively. The copolymerization in a comonomer feed ratio of 1/1 by complex **1** (0.5 mol%) and BnOH converted 94% $\text{rac-8DL}^{\text{Me}}$ to P3HB within 1 min, at which time the conversion of 7-HL just reached to 1.5% (run 1, Table 2), giving a copolymer with $M_n = 12.5$ kg/mol and $\mathcal{D} = 1.04$. Extending the copolymerization time to 30 min, the conversion of 7-HL achieved 100%, obtaining a copolymer with a higher molar mass of $M_n = 21.8$ kg/mol ($\mathcal{D} = 1.16$, run 2, Table 2). The kinetics of the copolymerization (Figure 3A) explicitly suggested that the polymerization rate of $\text{rac-8DL}^{\text{Me}}$ is significantly higher than that of 7-HL. These results indicated a block structure of the resulting copolymer, P3HB-*b*-P7HHp, albeit not a perfect block structure with some tapering, since a very small amount of 7-HL units got incorporated into the P3HB block (Figure 3A). However, at the 2/1 $\text{rac-8DL}^{\text{Me}}$ /7-HL feed ratio, block copolymer P3HB-*b*-P7HHp with non or negligible tapering phase can be produced (Figure 3B).

Similar conversion trends of both monomers were observed with the feed ratio of $[\text{rac-DL}^{\text{Me}} + 7\text{-HL}]/[\mathbf{1}] = 400/1$, affording block copolymer P3HB-*b*-P7HHp with a higher molar mass of $M_n = 32.0$ kg/mol ($\mathcal{D} = 1.16$, run 3, Table 2) after 60 min. The lanthanum analogue **2** with a larger ionic radius also exhibited similar catalytic behavior: $\text{rac-DL}^{\text{Me}}$ was converted to P3HB completely within 1 min, while 7-HL polymerization proceeded much more slowly, achieving 85% conversion after 120 min, and thus giving a block copolymer P3HB-*b*-P7HHp with high molar mass and narrow dispersities ($M_n = 53.6\text{--}124$ kg/mol, $\mathcal{D} = 1.01\text{--}1.15$; runs 3–6, Table 2). Varying the $\text{rac-8DL}^{\text{Me}}$ /7-HL feed ratio from 2/1 to 1/2, block copolymers with different relative block lengths were obtained (runs 7–8, Table 2). However, much lower molar mass ($M_n = 21.7\text{--}52.6$ kg/mol) and higher dispersities ($\mathcal{D} = 1.29\text{--}1.37$) of the resultant copolymers were observed, relative to that of the copolymer

TABLE 2 Results of copolymerizations of *rac*-DL^{Me} with 7-HL^a

Run	Cat	<i>rac</i> -DL ^{Me} /7-HL	[<i>rac</i> -DL ^{Me} + 7-HL]/[Cat]/[BnOH]	Time (min)	Conv. (%) ^b		<i>M</i> _{n,calcd} ^c (kg/mol)	<i>M</i> _n ^d (kg/mol)	<i>D</i> ^d (<i>M</i> _w / <i>M</i> _n)
					<i>rac</i> -DL ^{Me}	7-HL			
1	1	1/1	200/1/1	1	94	1.5	16.5	12.5	1.04
2	1	1/1	200/1/1	30	100	100	30.1	21.8	1.16
3	1	1/1	400/1/1	60	100	93	58.4	32.0	1.16
4	2	1/1	800/1/1	1	100	6.5	72.3	53.6	1.03
5	2	1/1	800/1/1	8	100	61	100	60.3	1.14
6	2	1/1	800/1/1	120	100	85	113	124	1.15
7	2	2/1	800/1/1	24 h	100	85	121	52.6	1.29
8	2	1/2	800/1/1	16 h	100	96	112	21.7	1.37

^aConditions: *rac*-DL^{Me} + 7-HL = 1.0 mmol, *V*_{solvent} = 1.0 mL, DCM as the solvent, BnOH as the initiator, the catalyst and initiator amount varied according to the [*rac*-DL^{Me} + 7-HL]/[Cat]/[BnOH] ratio, room temperature.

^bConversions of *rac*-DL^{Me} and 7-HL measured by ¹H NMR spectra of the quenched solution in benzoic acid/chloroform.

^c*M*_{n,calcd} = MW(7-HL) × [7-HL]/[cat] × conv (%) of 7-HL + MW(*rac*-DL^{Me}) × [*rac*-DL^{Me}]/[cat] × conv (%) of *rac*-DL^{Me} + MW of chain-end groups (BnOH).

^dWeight-average molar mass (*M*_w), number-average molar mass (*M*_n), and dispersities (*D* = *M*_w/*M*_n) determined by SEC coupled with an 18-angle light scattering detector at 40 °C in chloroform.

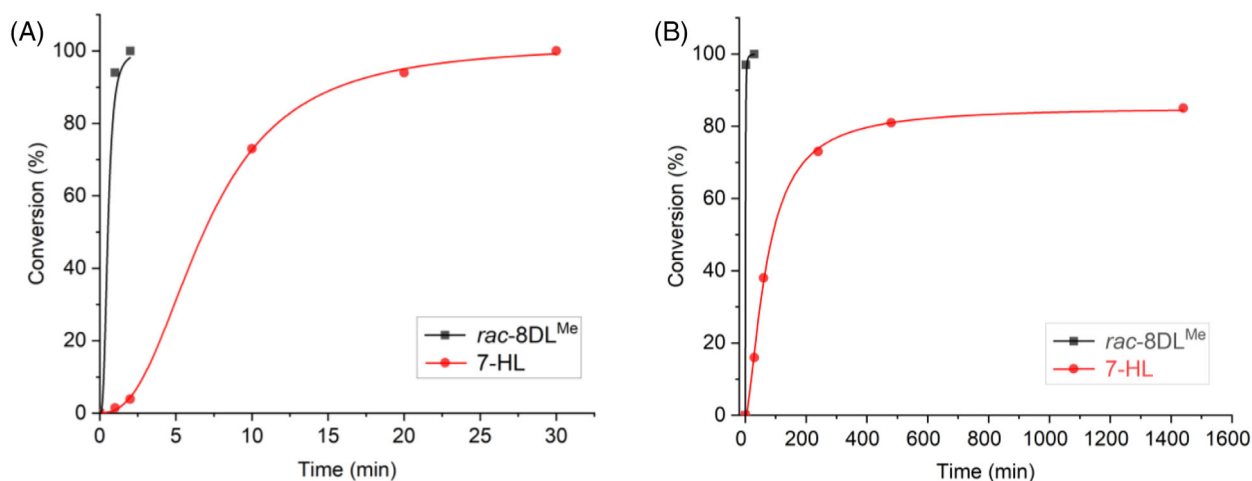


FIGURE 3 Time-conversion plots for the copolymerization of *rac*-8DL^{Me} and 7-HL: (A) by catalyst **1** with [*rac*-8DL^{Me} + 7-HL]/[**1**] = 200/1 and *rac*-8DL^{Me}/7-HL = 1/1 (run 2, Table 2), and (B) by catalyst **2** with [*rac*-8DL^{Me} + 7-HL]/[**1**] = 800/1 and *rac*-8DL^{Me}/7-HL = 2/1 (run 7, Table 2)

obtained with *rac*-8DL^{Me}/7-HL ratio of 1/1, presumably due to transesterification side reactions occurred after a long reaction time of 16–24 h. Noteworthy is that the *rac*-8DL^{Me}/7-HL copolymerization in a 2/1 feed ratio by catalyst **2** converted 97% *rac*-8DL^{Me} into P3HB in 2 min but at which time no conversion of 7-HL was observed (Figure 3B, run 7, Table S1), indicating that the resulting block copolymer had a negligible tapering phase.

Considering that the much higher polymerization rate of *rac*-8DL^{Me} than that of 7-HL led to the formation of block copolymer P3HB-*b*-P7HHp with the *rac*-8DL^{Me}/7-HL feed ratio from 2/1 to 1/2, a much lower feed ratio (i.e., higher 7-HL loading) must be employed to possibly obtain random copolymer P(3HB-*co*-7HHp).

In addition, to avoid the formation of block segments, the copolymerization must be terminated before reaching full conversion of *rac*-8DL^{Me}. From the polymerization results summarized in Table 3, when the polymerization time was extended from 10 min to 12 min, during which time the *rac*-DL^{Me} conversion was increased from 96 to 97%, the copolymerization of *rac*-8DL^{Me} and 7-HL in a 1/5 molar ratio and *rac*-8DL^{Me}/**1** = 200/1 gave random copolymers P(3HB-*co*-7HHp) with 7-HL incorporations ranging from 18.0 to 21.8% (runs 1–2, Table 3). The obtained P(3HB-*co*-7HHp) exhibited molar mass of 20.6–22.3 kg/mol and a narrow dispersity of 1.06. As expected, the random copolymer had only one *T*_m value between that of P3HB and P7HHp, ~154 °C. A copolymer with

TABLE 3 Results of random copolymerizations of *rac*-DL^{Me} with 7-HL^a

Run	Cat	[<i>rac</i> -DL ^{Me}]/[Cat]/[BnOH]	<i>rac</i> -DL ^{Me} /7-HL	Time (min)	Conv. of <i>rac</i> -DL ^{Me} (%) ^b	7-HL content ^c (%)	$M_{n,calcd}$ ^d (kg/mol)	M_n ^e (kg/mol)	\bar{D} ^e (M_w/M_n)	T_m ^f (°C)
1	1	200/1/1	1/5	10	96	18.0	38.6	20.6	1.06	154
2	1	200/1/1	1/5	12	97	21.8	40.4	22.3	1.06	153
3	1	200/1/1	1/10	20	92	29.8	41.8	18.5	1.05	139
4	1	400/1/1	1/5	50	93	11.1	70.1	31.2	1.04	154
5	1	400/1/1	1/10	18 h	73	17.2	58.2	21.7	1.04	141
6	1	600/1/1	1/5	24 h	71	5.8	76.8	25.4	1.05	156
7	2	400/1/1	1/5	2	97	6.9	70.6	32.6	1.04	164
8	2	400/1/1	1/10	5	81	6.1	58.6	19.3	1.08	160

^aConditions: *rac*-DL^{Me} = 0.8 mmol, $V_{solvent}$ = 0.8 mL, DCM as the solvent, BnOH as the initiator, the catalyst and initiator amount varied according to the [*rac*-DL^{Me}]/[Cat]/[BnOH] ratio, room temperature.

^bConversions of *rac*-DL^{Me} measured by ¹H NMR spectra of the quenched solution in benzoic acid/chloroform.

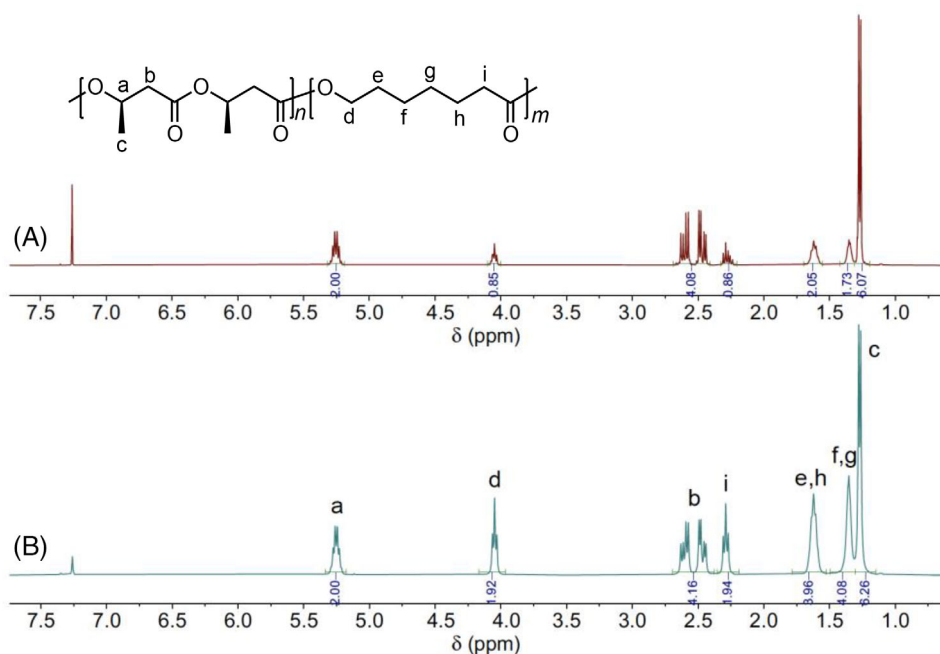
^c7-HL content measured by ¹H NMR of the isolated copolymer.

^d $M_{n,calcd}$ = MW(7-HL) × [7-HL]/[cat] × conv (%) of 7-HL + MW(*rac*-DL^{Me}) × [*rac*-DL^{Me}]/[cat] × conv (%) of *rac*-DL^{Me} + MW of chain-end groups (BnOH).

^eWeight-average molar mass (M_w), number-average molar mass (M_n), and dispersities (\bar{D} = M_w/M_n) determined by SEC coupled with an 18-angle light scattering detector at 40 °C in chloroform.

^fMeasured by DSC with the cooling and second heating rate of 10 °C/min.

FIGURE 4 ¹H NMR spectra (CDCl₃) of (A) random copolymer P(3HB-*co*-7HHp) with 7-HL incorporation of 29.8% (run 3, Table 3), and (B) block copolymer P3HB-*b*-P7HHp with P7HHp content of ~50% (run 2, Table 2)



higher 7-HL incorporation of 29.8% and thus correspondingly lower T_m of 139 °C was accessible via copolymerization with a lower *rac*-8DL^{Me}/7-HL feed ratio of 1/10 (M_n = 18.5 kg/mol, \bar{D} = 1.05; run 3, Table 3). To increase the molar mass of the resulting copolyester, lower catalyst concentrations ([*rac*-8DL^{Me}]/[cat] = 400/1–600/1) were employed to afford P(3HB-*co*-7HHp) with M_n = 25.4–31.2 kg/mol and \bar{D} = 1.04–1.05, but lower 7-HL incorporation of 5.8–17.2% (runs 4–6, Table 3). Switching to lanthanum complex **2** resulted in faster polymerizations but lower 7-HL contents (6.1–6.9%) in

the P(3HB-*co*-7HHp) copolymer (runs 7–8), which can be ascribed to its relatively more pronounced rate enhancement by catalyst **2** for *rac*-DL^{Me} than that for 7-HL.

2.3 | Microstructures and thermal and mechanical properties of copolyesters

The microstructures of the copolymers of *rac*-DL^{Me} with 7-HL were investigated by ¹H and ¹³C NMR methods. Figure 4 depicts ¹H NMR spectra of typical random

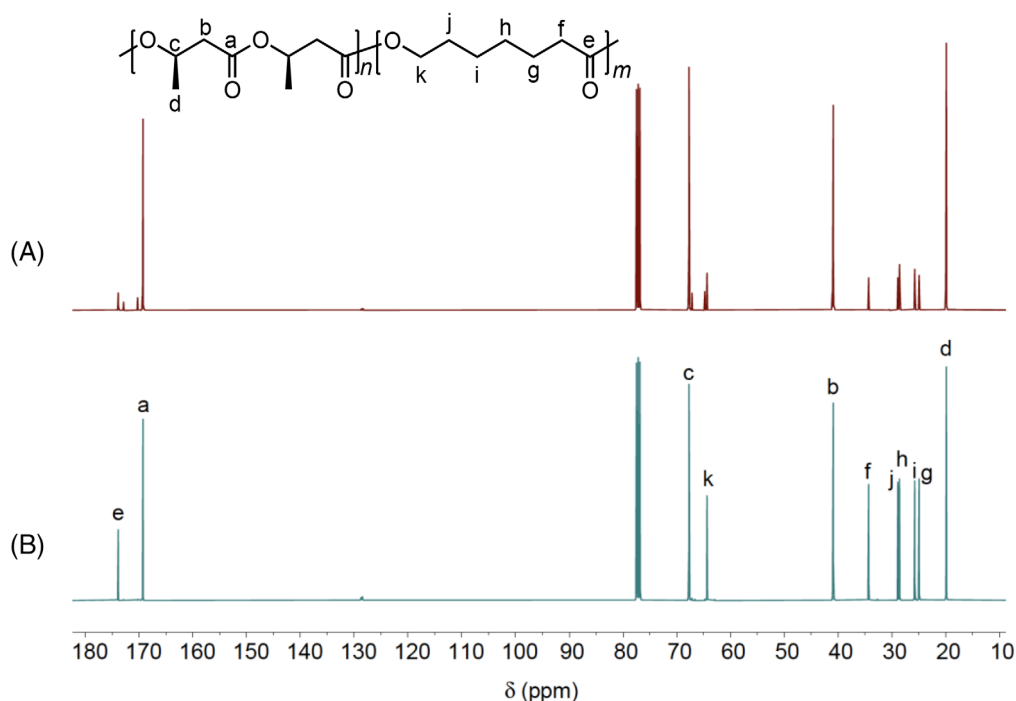


FIGURE 5 ^{13}C NMR spectra (CDCl_3) of (A) random copolymer P(3HB-co-7HHp) with 7-HL incorporation of 29.8% (run 3, Table 3), and (B) block copolymer P3HB-*b*-P7HHp with P7HHp content of ~50% (run 2, Table 2)

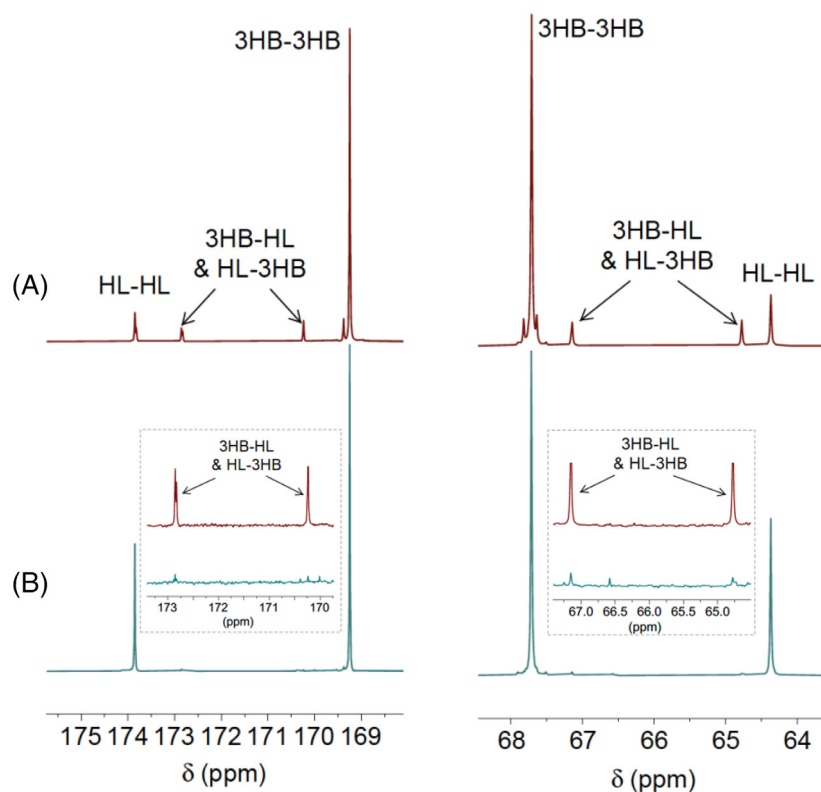


FIGURE 6 ^{13}C NMR spectra (CDCl_3) in carbonyl and oxygen-alkyl regions of (A) random copolymer P(3HB-co-7HHp) with 7-HL incorporation of 29.8% (run 3, Table 3), and (B) block copolymer P3HB-*b*-P7HHp with P7HHp content of ~50% (run 2, Table 2)

copolymer P(3HB-co-7HHp) and block copolymer P3HB-*b*-P7HHp, from which no difference could be observed besides the monomer incorporation or composition in the copolymer. On the other hand, ^{13}C NMR spectra

provided more detailed information about the microstructures (Figures 5–6). For the ^{13}C NMR spectrum (Figures 5–6A) of random copolymer P(3HB-co-7HHp), the expanded carbonyl resonances (169.2–173.8 ppm)

were resolved into four groups of peaks, arising from different diad sequences of 3HB and HL units (3HB-3HB, 169.2 ppm; 3HB-HL, 170.2 ppm; HL-3HB, 172.8 ppm; and HL-HL, 173.8 ppm). A similar resolution of resonances (64.4–67.7 ppm) for the carbon atom that linked to the oxygen atom was also observed. The presence of 3HB-HL and HL-3HB alternating sequences further confirmed the insertion of 7-HL into the resulting copolymer P(3HB-co-7HHp). Importantly, the carbonyl region of block copolymer P3HB-*b*-P7HHp in the ^{13}C NMR spectrum (Figures 5–6B) also showed the peaks for 3HB-HL and HL-3HB alternating sequences, but with much lower intensity, suggesting the copolymer is a block copolymer but not a mixture of P3HB and P7HHp. To provide further evidence for the formation of copolymer P3HB-*b*-P7HHp, not a mixture of P3HB and P7HHp, solvent extraction method was performed to isolate the possible potential mixture of P3HB and P7HHp. Since isotactic P3HB has poor solubility in tetrahydrofuran (THF) while P7HHp can dissolve in THF well, THF (80 mL) was utilized to extract the block copolymer P3HB-*b*-P7HHp (200 mg) prepared with $\text{rac-8DL}^{\text{Me}}/7\text{-HL} = 1/1$ and $[\text{rac-8DL}^{\text{Me}} + 7\text{-HL}]/[\mathbf{1}] = 200/1$ (run 2, Table 2). After stirring in THF for 8 h, 168 mg (84 wt%) of insoluble fraction was collected, which showed a similar ^1H NMR spectrum (Figure S2a) with the original polymer (Figure 4B). This result suggested the P7HHp was indeed covalently linked with P3HB, making it insoluble in THF. While the soluble fraction (16 wt%) showed a ^1H NMR spectrum (Figure S2b) with a much higher P7HHp content (97%), the presence of the long P7HHp block but short P3HB block segment made it soluble in THF. We also examined the block structure of P3HB-*b*-P7HHp by DOSY NMR analysis, the spectrum of which (Figure S3) showed a single diffusion coefficient for the observed signals, thus providing additional evidence for the block copolymer structure as a single component. These results confirmed that the resulting copolymer prepared with $\text{rac-8DL}^{\text{Me}}/7\text{-HL} = 1/1$ is indeed that of block copolymer.

The thermal properties of the block copolymer P3HB-*b*-P7HHp and random copolymers P(3HB-co-7HHp) were analyzed by DSC and TGA. When the copolymerization of $\text{rac-8DL}^{\text{Me}}$ and 7-HL (1/1) was terminated before generating the P7HHp block (run 1, Table 2), one crystalline temperature (T_c) of 79.0 °C and one T_m of 162 °C for the isotactic P3HB segments was observed on the first cooling and second heating scan of DSC curve (Figure S4a). After extending the polymerization time to full conversion of both monomers (run 2, Table 2), the resulting copolymer exhibited two T_m endotherm peaks at 64.8 and 162 °C (Figure 7A), corresponding to the P7HHp and P3HB block, respectively. Likewise, the block copolymer P3HB-*b*-P7HHp with a higher molar mass by catalyst

2 (run 6, Table 2) also showed two T_c values of 42.8 and 68.6 °C and two T_m values of 63.6 and 165 °C (Figure 7B). A similar pattern peaks on DSC curves (Figure S5) but with different relative intensity was observed with the block copolymers P3HB-*b*-P7HHp prepared with different $\text{rac-8DL}^{\text{Me}}/7\text{-HL}$ molar ratios of 2/1 and 1/2 (runs 8–9, Table 2).

For the random copolymers P(3HB-co-7HHp), generally, copolymers with higher 7-HL incorporations exhibited lower, but single, T_m values, as shown in Figures 8 and S6–S11. Noting that all the copolymers prepared with 8DL^{Me}/7-HL molar ratios of 1/5 by catalyst 1 showed a similar T_m of 153–156 °C (Figures 8A, S6–S7, and S9), although their 7-HL contents varied in a wide range. This observation indicated that higher 7-HL incorporation occurred at the late polymerization stage with lower $\text{rac-DL}^{\text{Me}}$ concentration, resulting in higher 7-HL incorporation at the end of the copolymer chain, which has little effect on the T_m value of the resulting copolymer. The copolymers obtained with $\text{rac-8DL}^{\text{Me}}/7\text{-HL}$ molar ratios of 1/10 by catalyst 1 exhibited lower T_m of 139–141 °C (Figures 8B and S8). In addition, the copolymers by catalyst 2 have lower 7-HL incorporations and thus higher T_m values of 160–164 °C (Figures S10–S11).

TGA and DTG curves (Figures 9A and S12) of block copolymers P(3HB-*b*-HL) prepared with different $\text{rac-8DL}^{\text{Me}}/7\text{-HL}$ molar ratios displayed two degradation steps, attributable to P3HB degradation at the lower initial degradation temperature and P7HHp degradation at the higher temperature. As expected, the ratio of the second degradation step contributed by P7HHp block increased with the decrease of the $\text{rac-8DL}^{\text{Me}}/7\text{-HL}$ molar ratio from 1/1 to 1/2, which was consistent with the P7HHp content in the block copolymer. On the other hand, random copolymer P(3HB-co-7HHp) prepared by $\text{rac-8DL}^{\text{Me}}/7\text{-HL} = 1/5$ with catalyst 2 and the 7-HL incorporation of 6.1 mol% (run 8, Table 3) showed one degradation step with T_d of 259 °C and T_{max} of 293 °C (Figure 9B), suggesting its random structure. However, for the copolymers with higher 7-HL incorporations prepared by catalyst 1, there was a small, second-degradation step occurred at higher temperature (Figures S13–15). This phenomenon was also observed in analogous random copolymers P(3HB-*b*-CL),⁶⁰ and it can be attributed to the fact that the higher 7-HL incorporation occurred at the later stage of the polymerization during the prolonged time with much lower $\text{rac-DL}^{\text{Me}}$ concentration. This scenario would produce the nonuniform copolymer chains, with much higher 7-HL incorporation at one end of the copolymer chain, accounting for the higher degradation temperature step.

Tensile testing of dog-bone-shaped P3HB-*b*-P7HHp (prepared by $[\text{rac-8DL}^{\text{Me}} + 7\text{-HL}]/[\mathbf{2}]/[\text{BnOH}] = 800/1/1$;

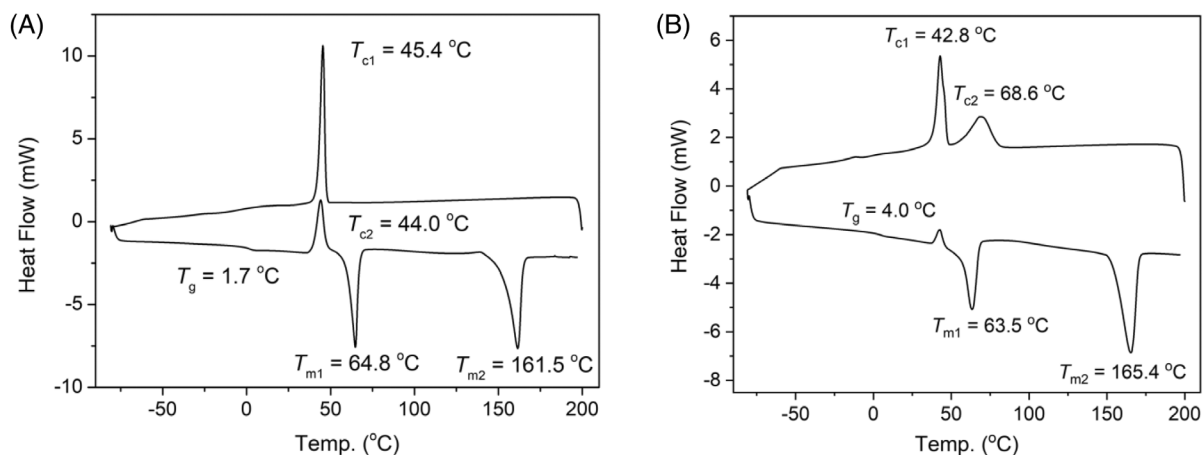


FIGURE 7 DSC curves of the block copolymers P3HB-*b*-P7HHp: (A) prepared by catalyst 1, P7HHp% = 50% (run 2, Table 2); and (B) prepared by catalyst 2, P7HHp% = 46% (run 6, Table 2)

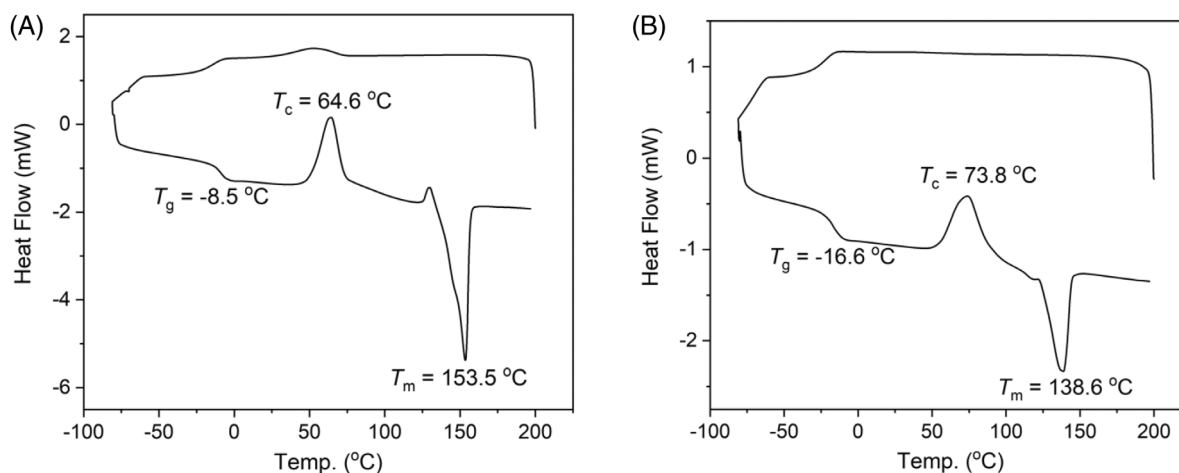


FIGURE 8 DSC curves of the random copolymers P(3HB-*co*-7HHp) produced by catalyst 1 with different 7-HL incorporations: (A) P7HHp% = 18.0% (run 1, Table 3); and (B) P7HHp% = 29.8% (run 3, Table 3)

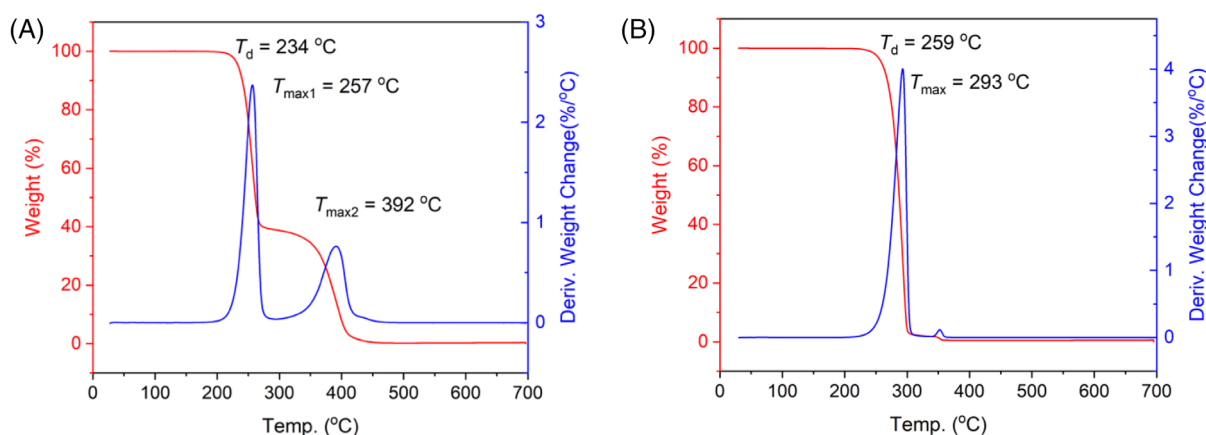


FIGURE 9 TGA (red) and DTG (blue) curves of (A) block copolymer P3HB-*b*-P7HHp (P7HHp% = 44 mol%; run 6, Table 2) and (B) the random copolymer P(3HB-*co*-7HHp) with 7-HL incorporation of 6.1 mol% (run 8, Table 3). Both copolymers shown here were produced by catalyst 2

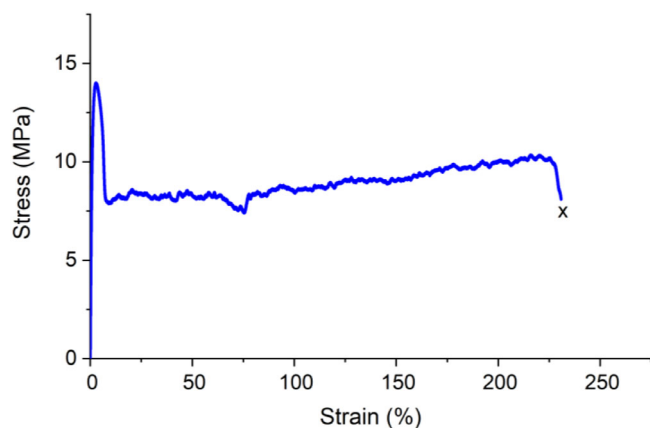


FIGURE 10 Stress–strain curve (10 mm/min, ambient temperature) of P3HB-*b*-P7HHp prepared with [*rac*-8DL^{Me} + 7-HL]/[2]/[BnOH] = 800/1/1 (run 6, Table 2). Break point indicated by “x”

run 6, Table 2) and P(3HB-*co*-7HHp) (prepared by [*rac*-8DL^{Me}]/[1]/[BnOH] = 200/1/1 and *rac*-8DL^{Me}/7-HL = 1/5; run 2, Table 3) specimens were performed to characterize their mechanical performance. From the stress/strain curve (Figure 10) of P3HB-*b*-P7HHp, it exhibited an σ_B of 14.0 MPa, E of 1.52 GPa, and ϵ_B of 231%, suggesting a comparably high Young's modulus but a much larger elongation at break as compared to isotactic P3HB ($E \sim 3$ GPa, $\epsilon_B \sim 3\%$),⁴¹ and higher Young's modulus than P7HHp. Therefore, the block copolymer P3HB-*b*-P7HHp can combine the advantages of high Young's modulus of isotactic P3HB and large elongation at break of P7HHp, making it a hard and tough plastic. However, the random copolymer P(3HB-*co*-7HHp) (Figure S23) just showed a comparable ultimate tensile strength of 11.9 MPa, but a much lower Young's modulus of 486 MPa and elongation at break of only 8.4%, due to its lower molar mass ($M_n \sim 20$ kg/mol) and 7-HL content ($\sim 20\%$).

3 | CONCLUSIONS

The eight-membered lactone 7-HL was studied for the first time via metal-catalyzed coordinative-insertion polymerization, achieving semi-crystalline P7HHp with a T_m of 68 °C, which is ~ 10 °C higher than PCL derived from the seven-membered lactone. Notably, P7HHp is shown to be a hard and tough plastic with an ultimate tensile strength of 35.3 ± 2.8 MPa, Young's modulus of 628 ± 4 MPa, and elongation at break of $672 \pm 49\%$. This lactone can be readily copolymerized with *rac*-8DL^{Me} to produce block copolymer P3HB-*b*-P7HHp or random copolymer P(3HB-*co*-7HHp) in a one-pot fashion, depending on the polymerization conditions, particularly the *rac*-8DL^{Me}/7-HL molar feed ratio. When the

copolymerization was conducted with the feed ratio from 2/1 to 1/2, block copolymer P3HB-*b*-P7HHp with M_n up to 124 kg/mol and $\bar{D} = 1.15$ was obtained, owing to catalyst's strong kinetic preference for polymerizing *rac*-8DL^{Me} over 7-HL. On the other hand, random copolymer P(3HB-*co*-7HHp) was produced with the feed ratio of 1/5 \sim 1/10, when the copolymerization was quenched before reaching full conversion of *rac*-8DL^{Me}. The 7-HL incorporation into the random copolymer can be tuned from 6.1 to 29.8%, giving random copolymers P(3HB-*co*-7HHp) with $T_m = 139$ –164 °C, $M_n = 18.5$ –32.6 kg/mol, and $\bar{D} = 1.04$ –1.08.

All block copolymers, P3HB-*b*-P7HHp, display two crystallization temperatures and thus exhibit two crystalline domains with the first T_m around 65 °C for the P7HHp block and the second T_m around 162–167 °C for the isotactic P3HB block. In addition, block copolymers also display two degradation steps, corresponding to the P3HB block degradation at a lower initial degradation temperature ($T_d \sim 234$ °C) and the P7HHp block degradation at a higher temperature ($T_d \sim 390$ °C). In contrast, random copolymer P(3HB-*co*-7HHp) shows only one T_c and one T_m , the values of which are dependent on the *rac*-8DL^{Me}/7-HL feed ratio and thus 7-HL incorporation in the copolymer, and displays one degradation step with a T_d of 232–259 °C and a T_{max} of 259–293 °C. Notably, the block copolymer P3HB-*b*-P7HHp is a hard and tough plastic with an ultimate tensile strength of 14.0 MPa, Young's modulus of 1.52 GPa, and elongation at break of 231%. Therefore, the block copolymer combines the advantages of high modulus of isotactic P3HB and large elongation at break of P7HHp.

ACKNOWLEDGMENTS

This work was supported by the US National Science Foundation (NSF-1955482) to E.Y.-X.C. and the National Natural Science Foundation of China (52173093) and Peking University Ge Li and Ning Zhao Life Science Research Fund for Young Scientists to X.T.

ORCID

Xiaoyan Tang  <https://orcid.org/0000-0002-0050-6699>

Eugene Y.-X. Chen  <https://orcid.org/0000-0001-7512-3484>

REFERENCES

- [1] A. L. Sisson, M. Schroeter, A. Lendlein, *Handbook of Biodegradable Polymers*, Wiley-VCH Verlag, Weinheim, Germany, 2011, p. 1. <https://doi.org/10.1002/9783527635818.ch1>
- [2] M. M. Reddy, S. Vivekanandhan, M. Misra, S. K. Bhatia, A. K. Mohanty, *Prog. Polym. Sci.* 2013, 38, 1653.
- [3] A. C. Albertsson, I. K. Varma, in *Degradable Aliphatic Polyesters*, Vol. 157 (Ed: A. C. Albertsson) Springer, Berlin, Heidelberg, 2002, p. 1. https://doi.org/10.1007/3-540-45734-8_1

- [4] A. Larrañaga, E. Lizundia, *Eur. Polym. J.* **2019**, *121*, 109296.
- [5] L. Al-Shok, D. M. Haddleton, F. Adams, *Advances in Polymer Science*. Springer Berlin Heidelberg, Berlin, Heidelberg, pp. 1–71. https://doi.org/10.1007/12_2021_111
- [6] X. Tang, *Advances in Polymer Science*. Springer Berlin Heidelberg, Berlin, Heidelberg, pp. 1–21. https://doi.org/10.1007/12_2022_119
- [7] X. Tang, E. Y.-X. Chen, *Chem* **2019**, *5*, 284.
- [8] D. M. Lyubov, A. O. Tolpygin, A. A. Trifonov, *Coord. Chem. Rev.* **2019**, *392*, 83.
- [9] J.-F. Carpentier, *Organometallics* **2015**, *34*, 4175.
- [10] J.-F. Carpentier, *Macromol. Rapid Commun.* **2010**, *31*, 1696.
- [11] C. M. Thomas, *Chem. Soc. Rev.* **2010**, *39*, 165.
- [12] O. Dechy-Cabaret, B. Martin-Vaca, D. Bourissou, *Chem. Rev.* **2004**, *104*, 6147.
- [13] M. Okada, *Prog. Polym. Sci.* **2002**, *27*, 87.
- [14] P. Lecomte, C. Jérôme, in *Synthetic Biodegradable Polymers* (Eds: B. Rieger, A. Künkel, G. W. Coates, R. Reichardt, E. Dinjus, T. A. Zevaco), Springer Berlin Heidelberg, Berlin, Heidelberg **2012**, p. 173.
- [15] M. K. Kiesewetter, E. J. Shin, J. L. Hedrick, R. M. Waymouth, *Macromolecules* **2010**, *43*, 2093.
- [16] N. E. Kamber, W. Jeong, R. M. Waymouth, R. C. Pratt, B. G. G. Lohmeijer, J. L. Hedrick, *Chem. Rev.* **2007**, *107*, 5813.
- [17] S. Kobayashi, *Polym. Adv. Technol.* **2015**, *26*, 677.
- [18] Q. Song, C. Pascouau, J. Zhao, G. Zhang, F. Peruch, S. Carloti, *Prog. Polym. Sci.* **2020**, *110*, 101309.
- [19] M. A. Hillmyer, W. B. Tolman, *Acc. Chem. Res.* **2014**, *47*, 2390.
- [20] H. Li, R. M. Shakaroun, S. M. Guillaume, J.-F. Carpentier, *Chem. – Eur. J.* **2020**, *26*, 128.
- [21] A. Amgoune, C. M. Thomas, S. Ilinca, T. Roisnel, J.-F. Carpentier, *Angew. Chem. Int. Ed.* **2006**, *45*, 2782.
- [22] A. Amgoune, C. M. Thomas, T. Roisnel, J.-F. Carpentier, *Chem. – Eur. J.* **2006**, *12*, 169.
- [23] N. Ajellal, M. Bouyahyi, A. Amgoune, C. M. Thomas, A. Bondon, I. Pillin, Y. Grohens, J.-F. Carpentier, *Macromolecules* **2009**, *42*, 987.
- [24] M. Bouyahyi, N. Ajellal, E. Kirillov, C. M. Thomas, J.-F. Carpentier, *Chem. – Eur. J.* **2011**, *17*, 1872.
- [25] S. Bloembergen, D. A. Holden, T. L. Bluhm, G. K. Hamer, R. H. Marchessault, *Macromolecules* **1989**, *22*, 1656.
- [26] C. Jaimes, M. Arcana, A. Brethon, A. Mathieu, F. Schue, J. M. Desimone, *Eur. Polym. J.* **1998**, *34*, 175.
- [27] B. Wu, R. W. Lenz, *Macromolecules* **1998**, *31*, 3473.
- [28] A. Le Borgne, N. Spassky, *Polymer* **1989**, *30*, 2312.
- [29] M. Zintl, F. Molnar, T. Urban, V. Bernhart, P. Preishuber-Pflügl, B. Rieger, *Angew. Chem. Int. Ed.* **2008**, *47*, 3458.
- [30] N. Ajellal, G. Durieux, L. Delevoye, G. Tricot, C. Dujardin, C. M. Thomas, R. M. Gauvin, *Chem. Commun.* **2010**, *46*, 1032.
- [31] Z. Zhuo, C. Zhang, Y. Luo, Y. Wang, Y. Yao, D. Yuan, D. Cui, *Chem. Commun.* **2018**, *54*, 11998.
- [32] Z. Li, J. Yang, X. J. Loh, *NPG Asia Mater.* **2016**, *8*, e265.
- [33] A. Anjum, M. Zuber, K. M. Zia, A. Noreen, M. N. Anjum, S. Tabasum, *Int. J. Biol. Macromol.* **2016**, *89*, 161.
- [34] S. Muhammadi, M. Afzal, S. Hameed, *Green Chem. Lett. Rev.* **2015**, *8*, 56.
- [35] M. N. Somleva, O. P. Peoples, K. D. Snell, *Plant Biotechnol. J.* **2013**, *11*, 233.
- [36] B. Laycock, P. Halley, S. Pratt, A. Werker, P. Lant, *Prog. Polym. Sci.* **2013**, *38*, 536.
- [37] S. Taguchi, T. Iwata, H. Abe, Y. Doi, in *Polymer Science: A Comprehensive Reference* (Eds: K. Matyjaszewski, M. Möller), Elsevier, Amsterdam **2012**, p. 157.
- [38] G.-Q. Chen, in *Plastics from Bacteria: Natural Functions and Applications*, Vol. 14 (Ed: G.-Q. Chen), Springer-Verlag, Berlin **2010**, p. 17.
- [39] G.-Q. Chen, *Chem. Soc. Rev.* **2009**, *38*, 2434.
- [40] R. W. Lenz, R. H. Marchessault, *Biomacromolecules* **2005**, *6*, 1.
- [41] K. Sudesh, H. Abe, Y. Doi, *Prog. Polym. Sci.* **2000**, *25*, 1503.
- [42] Y. Poirier, C. Nawrath, C. Somerville, *Nat. Biotechnol.* **1995**, *13*, 142.
- [43] H.-M. Müller, D. Seebach, *Angew. Chem. Int. Ed. Engl.* **1993**, *32*, 477.
- [44] X. Tang, E. Y.-X. Chen, *Nat. Commun.* **2018**, *9*, 2345.
- [45] X. Tang, A. H. Westlie, E. M. Watson, E. Y.-X. Chen, *Science* **2019**, *366*, 754.
- [46] X. Tang, A. H. Westlie, L. Caporaso, L. Cavallo, L. Falivene, E. Y.-X. Chen, *Angew. Chem. Int. Ed.* **2020**, *59*, 7881.
- [47] A. H. Westlie, E. Y.-X. Chen, *Macromolecules* **2020**, *53*, 9906.
- [48] M. Hong, E. Y.-X. Chen, *Nat. Chem.* **2016**, *8*, 42.
- [49] M. Labet, W. Thielemans, *Chem. Soc. Rev.* **2009**, *38*, 3484.
- [50] S. M. Guillaume, E. Kirillov, Y. Sarazin, J.-F. Carpentier, *Chem. – Eur. J.* **2015**, *21*, 7988.
- [51] U. Piotrowska, M. Sobczak, *Molecules* **2015**, *20*, 1.
- [52] S. Dagherne, M. Normand, E. Kirillov, J.-F. Carpentier, *Coord. Chem. Rev.* **2013**, *257*, 1869.
- [53] A. K. Sutar, T. Maharana, S. Dutta, C.-T. Chen, C.-C. Lin, *Chem. Soc. Rev.* **2010**, *39*, 1724.
- [54] S. Agarwal, C. Mast, K. Dehnicke, A. Greiner, *Macromol. Rapid Commun.* **2000**, *21*, 195.
- [55] X. Li, C. Chen, J. Wu, *Molecules* **2018**, *23*, 189.
- [56] T. Fuoco, D. Pappalardo, *Catalysts* **2017**, *7*, 64.
- [57] L. van der Mee, F. Helmich, R. de Bruijn, J. A. J. M. Vekemans, A. R. A. Palmans, E. W. Meijer, *Macromolecules* **2006**, *39*, 5021.
- [58] X. Tang, M. Hong, L. Falivene, L. Caporaso, L. Cavallo, E. Y.-X. Chen, *J. Am. Chem. Soc.* **2016**, *138*, 14326.
- [59] M. Hong, E. Y.-X. Chen, *Macromolecules* **2014**, *47*, 3614.
- [60] X. Tang, C. Shi, Z. Zhang, E. Y.-X. Chen, *Macromolecules* **2021**, *54*, 9401.

SUPPORTING INFORMATION

Additional supporting information can be found online in the Supporting Information section at the end of this article.

How to cite this article: X. Tang, C. Shi, Z. Zhang, E. Y.-X. Chen, *J. Polym. Sci.* **2022**, *60*(24), 3478. <https://doi.org/10.1002/pol.20220418>